Available online at www.sciencedirect.com

ScienceDirect

Procedia Materials Science 3 (2014) 122 – 128

Procedia Materials Science

www.elsevier.com/locate/procedia

20th European Conference on Fracture (ECF20)

Modeling and experimental study of long term creep damage in austenitic stainless steels

Y.CUI[a,b,*], M. SAUZAY[a], C. CAES[a], P. BONNAILLIE[c], B. ARNAL[d]

[a]*CEA, DEN, SRMA, LC2M, F-91191 Gif-sur-Yvette, France*
[b]*Université Paris 6 Pierre et Marie Curie, 75005 Paris, France*
[c]*CEA, DEN, SRMP, F-91191 Gif-sur-Yvette, France*
[d]*CEA, DEN, SRMA, LA2M, F-91191 Gif-sur-Yvette, France*

Abstract

Different batches of austenitic stainless steels (316LN) are subjected to numerous creep tests carried out at various stresses and temperatures between 525°C to 750°C up to nearly $50 \bullet 10^3$h. Interrupted creep tests show an acceleration of the creep deformation only during the last 15% of creep lifetime which corresponds to macroscopic necking. The modeling of necking using the Norton flow law allows lifetime predictions in fair agreement with experimental data up to a few thousand hours only. In fact, the experimental results show that, the extrapolation of the 'stress – lifetime' curves obtained at high stress leads to large overestimations of lifetimes at low stress. After FEG–SEM observations, these overestimates are mainly due to additional intergranular cavitation along grain boundaries as often observed in many metallic materials. The modeling of cavity growth by vacancy diffusion along grain boundaries coupled with continuous nucleation proposed by Riedel is carried out. For each specimen, ten FEG–SEM images (about 250 observed grains) are analyzed to determine the rate of cavity nucleation assumed to be constant during each creep test in agreement with many literature results. This constant rate is the only measured parameter which is used as input of the Riedel model. Lifetimes for long term creep are rather fairly well predicted by either the necking model or the Riedel model with respect to experimental lifetimes up to 200000 hours for temperatures between 525°C and 700°C. A transition time as well as a transition stress is defined by the intersection of the lifetime curves based on the necking and Riedel modellings. This is due to a change in damage mechanism. The scatter in lifetimes predicted by the Riedel model induced by the uncertainly of some parameter values is around 50%. This model is also validated for martensitic steels (Lim et al, 2011.) and for other austenitic SSs 304H, 316H, 321H (creep rupture data provided by Dr. F. Abe, NIMS). A transition from

* Corresponding author. Tel.: +33-(0)1-69-08-67-26; fax: +33-(0)1-69-08-71-67.
E-mail address: Yiting.cui@cea.fr

Selection and peer-review under responsibility of the Norwegian University of Science and Technology (NTNU), Department of Structural Engineering
doi:10.1016/j.mspro.2014.06.023

power-law to viscous creep behavior is reported in the literature at 650°C–750°C. It allows us to predict even better lifetimes up to 200000 hours at very high temperature.

Selection and peer-review under responsibility of the Norwegian University of Science and Technology (NTNU), Department of Structural Engineering

Keywords: Austenitic stainless steels (SSs); long term creep; necking; intergranular damage; cavity nucleation; cavity growth; grain boundary diffusion.

1. Introduction

The present study of austenitic stainless steels (SSs) is mainly focused on the family of low-carbon and nitrogen-strengthened steels called 316L(N). Multi-batch creep data are provided by CEA, EDF, Creusot-Loire (1987), by the National Institute for Materials Science, Japan, NIMS (1997 & 2013) and by the study of Brinkman (2001). The creep lifetimes of some IVth generation reactors components in austenitic stainless steels require on the one hand to carry out very long term creep tests (>20years) and on the other hand to understand and to model the damage mechanisms in order to propose physically-based extrapolations towards 60 years of service. Two fracture mechanisms are in fact involved during creep rupture tests, depending on stress, temperature and lifetime: either necking or intergranular cavity nucleation and growth (Auzoux (2004)).

The lifetime model was developed by Hart (1967) to account for creep damage by necking, which was first studied by Considère (1885) and more recently by Dumoulin et al. (2003). For viscoplastic materials, this model obeys the Norton power-law equation. The reduction in cross-section at fracture is studied in order to define the failure criterion. It predicts the creep curves and the creep to failure time of steels at various temperatures at least for most stress levels. Extensive necking leads to large overestimations of long term creep lifetimes. Therefore, the necking model is used only for predict short to medium term creep fracture. The next step is to include intergranular damage in the fracture modeling (Morris et al. (1978) or Yoshida (1985)). Fracture of long-term creep specimens is governed by diffusional growth and coalescence of intergranular cavities. Creep cavities along coarse intergranular carbides or other inter-metallic phases, and "triple point cracks" at grain boundary intersections are observed by SEM-FEG. Hence, these observations allow us to validate the hypothesis of dominant intergranular damage.

Experimental 'creep failure stress - lifetime' curves are plotted for tests carried out at temperatures between 500°C and 750°C. The extrapolation of the data obtained at high stress leads to overestimated lifetimes at low stress which differ by a factor of five with respect to experimental data. A model based on the continuous nucleation and growth of cavities by vacancy diffusion has been adapted from the work of Riedel (1987). According to numerous measurements carried out after interrupted tests, Dyson (1983) suggested that the cavities nucleate at a constant rate during each creep, $\dot{N}_0$ which is proportional to the minimum creep strain rate, $\dot{\varepsilon}_{min}$, with a pre-factor denoted as α'. Experimental results from a database of nineteen creep tests carried out up to failure on 316L(N) SSs at CEA/SRMA and EDF are examined so as to determine experimentally at various stresses and temperatures this parameter, α', which is used in the Riedel model.

These two fracture models are used in order to compare the predicted creep lifetimes with the experimental creep results at temperatures between 525 and 700°C. Thus, validation of this new prediction technique requires evidence if its applicability to a wide range of stainless steels.

Nomenclature

t_R	time to rupture
t_{min}	time at which the minimum creep strain rate $\dot{\varepsilon}_{min}$ is reached
ε_{min}	strain at which the minimum creep strain rate $\dot{\varepsilon}_{min}$ is reached
δD_r	initial variation in diameter divided by the average diameter of the specimen
N	exponent of the Norton power-law
$\dot{N}_0$	cavity nucleation rate (nucleation of cavities par unit grain boundary area and per unit time)
α'	factor of proportionality

N_m	number of cavities per unit area of polished section
N_a	number of cavities per unit grain boundary area
d_g	average diameter of austenitic grains
d_H	harmonic mean of intersected cavity diameter
ε_{fin}	final strain of the homogeneous areas of the specimens

2. Experimental procedures

The materials used in this study are 316L(N) stainless steels produced by Creusot-Loire. The chemical composition requirements are shown in table 1. The Creusot-Loire plates were heat treated at about 1100°C for about 1h followed by water quenching. Long-term tensile creep tests have been conducted to failure at temperatures between 500°C and 750°C for a large range of applied stresses. These tests have been carried out at CEA/SRMA, EDF and Creusot-Loire (Unirec) laboratories.

The creep-ruptured specimens were cut longitudinally and transversally using a water-cooled fine cutter, embedded in conductive resin and polished on emery papers and on buffing cloths with paste. The polishing on emery papers was carried out in the following order: grade180 (containing SiC particles of 100μm), grade 240 (80μm), grade 320 (60μm) and grade 600 (30μm). The final polishing on buffing cloths was carried out in the following order: buffing cloths with paste containing 9μm, 3μm and 1μm diamond particles. At the end, the samples were polished using a colloidal silica solution. The samples were examined by Field Emission Gun - Scanning Electron Microscopy (FEG-SEM) and optical microscopy. The observation areas were located far from the necking section, as shown in figure 1. For each specimen, ten FEG-SEM micrographs (Fig. 2a, about 250 observed grains) with magnification X500 were analyzed to determine the number of cavities per unit area of polished section, using the image processing software (NOESIS-Visilog 7.0).

Table 1. Chemical composition requirements of the 316L(N) plates produced by Creusot-Loire.

Element in wt.%								
C	Ni	Cr	Mo	Si	Mn	N	S	P
<0.03	12–12.5	17–18	2.3–2.7	<0.5	1.6–2	0.06–0.08	<0.025	<0.035

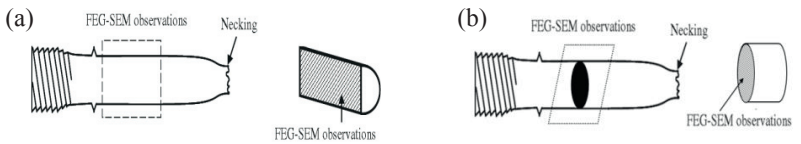

Fig. 1. Schematic sketches showing the sectioning procedure and areas used for FEG-SEM observations: (a) longitudinal sectioning; (b) transversal sectioning.

3. Necking evolutions

Necking is a first failure mechanism which is preeminent for short term creep. At any given time, a small portion of the gauge length is assumed to have a cross-section differing by a small amount, δS, from the whole gauge length, which is supposed to have a homogeneous cross-section, S. According to Hart's definition, Hart (1967), the deformation is unstable if this difference in cross-section increases with time. Using the volume conservation assumption, the Hart instability criterion is deduced which allows the prediction of the onset of necking. Predictions using this criterion show that necking starts just slightly later than t_{min}, time at which the minimum creep strain rate, $\dot{\varepsilon}_{min}$, is reached. By combining 'the Norton power law written in terms of true strain and stress and the cross-section evolutionary computation after the onset of necking', time to failure, Lim et al. (2011), is expressed as:

$$t_R - t_{\min} = \frac{1}{N \cdot \dot{\varepsilon}_{\min}} \left\{ \left(1 - \delta D_r \cdot \left(2 + \varepsilon_{\min}\right)\right)^N \right\} \quad (1)$$

With t_R (time to rupture), ε_{min} (strain at which the minimum creep strain rate $\dot{\varepsilon}_{min}$ is reached), N (exponent of the Norton power-law) and δD_r(initial variation in diameter divided by the average diameter of the specimen). The creep lifetime is computed taking into account the scatter in parameter values for temperatures between 525°C and 700°C with $\frac{t_{min}}{t_R} \in [0.1; 0.3]$; $\varepsilon_{min} \in [0.8\%; 3.5\%]$; $N \in [6; 20]$ and $\delta D_r \in [10^{-4}; 5 \cdot 10^{-3}]$.

Time to rupture, bounded by the lower and upper bound, allow us to predict correctly the creep lifetimes up to a few thousand hours for the considered temperature range; however, it leads to large overestimations as considering of long term creep. Following the literature, the intergranular cavity nucleation and growth might affect the time to fracture (Riedel (1987)).

4. Intergranular damage evolutions

As we have checked that the ratio between 'the radius of the cavities (diameter of observed cavities $\geqslant$ 100nm)' and 'the Rice length' is lower than 0.2 (criterion suggested by Needleman and Rice (1980)). We may assure that cavity growth is controlled by diffusion alone and growth by viscoplasticity can be neglected. Therefore, cavity growth is assumed to occur by vacancy diffusion so as to predict the mechanism of intergranular damage for the long term creep lifetimes of austenitic SSs. After FEG-SEM observations, the formation of intergranular creep cavities along grain boundaries is always observed for long term creep in both cross-sections and longitudinal-sections. According to numerous measurements carried out during the interrupted creep test specimens, Dyson 1983 suggested that cavities nucleate at a constant rate during creep tests, $\dot{N}_0$. It is defined as the number of cavities nucleated per unit grain boundary area and per unit time and given by:

$$\dot{N}_0 = \alpha' \cdot \dot{\varepsilon}_{\min} \quad \text{with} \quad \alpha' = \frac{N_a}{\varepsilon_{fin}} \text{ and } N_a = \frac{d_g \cdot N_m}{\pi \cdot d_H} \quad (2)$$

For various stress and temperature values, the parameter α' is evaluated using the image processing software of FEG-SEM micrographs which allows us to measure the number of cavities per unit area of polished section, N_m. The number of cavities per unit grain boundary area, N_a, is then deduced using Eq. 2. In Eq. 2, α' is a factor of proportionality which may vary widely from one material to another one. For the 316L(N) SS studied, the measured values of α' vary between $1.69 \cdot 10^9$ m^{-2} and $9.55 \cdot 10^9$ m^{-2} for temperatures between 525°C and 700°C.

Cavity growth by vacancy diffusion along grain boundaries coupled with continuous nucleation was modeled by Riedel (1987). Two bound curves predicting failure times have been deduced from the whole set of equations of the Riedel model by Lim (2011) improving the ones proposed by Riedel. The upper and lower bounds of the time to failure can be computed as:

$$0.301 \cdot \left(\frac{h(\alpha) k_b T}{\Omega D_b \delta \Sigma_n} \right)^{\frac{2}{5}} \frac{\left(\bar{\omega}\right)^{0.5164}}{\left(\dot{N}_0\right)^{\frac{3}{5}}} \leq t_R \leq 0.354 \cdot \left(\frac{h(\alpha) k_b T}{\Omega D_b \delta \Sigma_n} \right)^{\frac{2}{5}} \frac{\left(\bar{\omega}\right)^{\frac{2}{5}}}{\left(\dot{N}_0\right)^{\frac{3}{5}}} \quad (3)$$

Table 2 shows the different parameters used in the Riedel model equation with $D_b\delta$ the self-diffusion coefficient along grain boundaries times the grain boundary thickness δ (Eq. 4) and $h(\alpha)$ the cavity volume divided by volume of a sphere of the same radius (Eq. 5) where $F_v(\alpha)$ is a geometry function and α is the angle formed at the junction of a void and the grain boundary.

$$D_b\delta = D_b^0\delta \exp\left(-\frac{Q_b}{RT}\right) \quad (4)$$

$$\cos(\alpha)=\frac{\gamma_b}{2\gamma_s};\quad F_v(\alpha)=\frac{2\pi}{3}\cdot\left(2-3\cos(\alpha)+\cos(\alpha)^3\right);\quad h(\alpha)=\frac{3F_v(\alpha)}{4\pi\sin(\alpha)^3}=0.836\pm0.139 \quad (5)$$

Table 2. Parameters used in the Eq. 3. allowing the computation of the time to failure due to intergranular damage.

Parameter	Notation	Values
Ω	Atomic volume, m^3	$1.21\cdot10^{-29}$ (Riedel, 1987)
$D_b^0\delta$	Self-diffusion coefficient along grain boundaries times the grain boundary thickness δ, $m^3.s^{-1}$	$(5.3\pm1.4)\cdot10^{-13}$ (Perkins et al. 1973)
Q_b	Activation Energy for grain boundary self-diffusion, kJ/mol	177 ± 17 (Perkins et al. 1973)
γ_s	Surface free energy, J/m²	[2; 3] (Riedel, 1987)
γ_b	Grain boundary surface energy, J/m²	[0.1; 1.2] (Riedel, 1987)
$h(\alpha)$	Cavity volume divided by the volume of a sphere of the same radius	0.836 ± 0.139 (Raj and Ashby, 1975)
$\overline{\omega}_f$	Critical area fraction of creep cavities along grain boundaries	0.04 ± 0.01 (Auzoux, 2004)
α'	Cavity nucleation rate, m^{-2}	$[1.69\cdot10^9; 9.55\cdot10^9]$

Experimental and predicted rupture lifetimes at 650°C are plotted in Fig. 2b. A more global comparison between experimental lifetimes and the lifetimes predicted by the necking and the Riedel models is shown in Fig. 3a. Lifetimes are predicted fairly well for long term creep failure for temperatures between 525°C to 650°C. For very long term creep tests (>10^5h), at 700°C, the Riedel model overestimates lifetimes at low stress. The scatter in lifetimes predicted by the Riedel model is around 50%. As can be seen in Fig. 3b, a transition time may be defined as the intersection of the necking and Riedel lifetime curves at each temperature. The transition is due to a change in damage mechanism. This transition time corresponds fairly well to that observed on the experimental curves. The factor between experimental and predicted values is lower than 1.5.

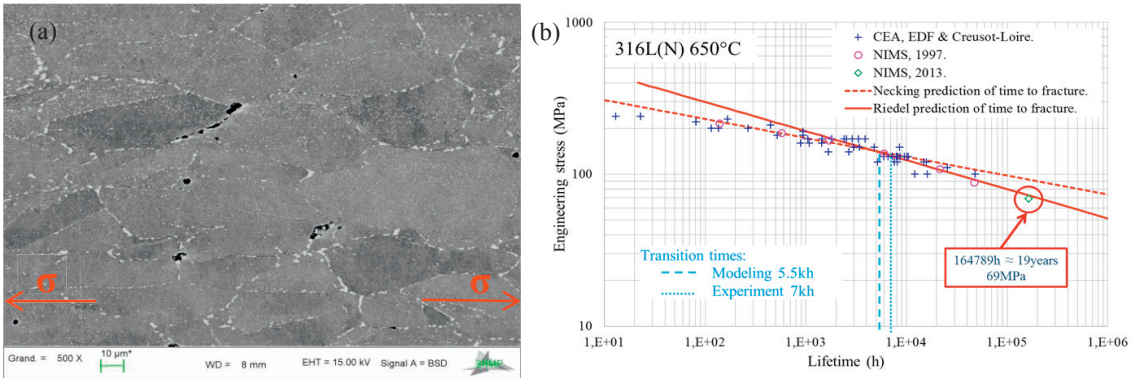

Fig. 2. (a) FEG-SEM image with magnification X500 (CEA/SRMP), Creep test at 700°C, 100MPa leading to failure after 2226h. (b) Experimental lifetimes and lifetimes predicted by either the necking model or the Riedel model at 650°C (CEA/SRMA, EDF & Creusot-Loire, NIMS (1997&2013)).

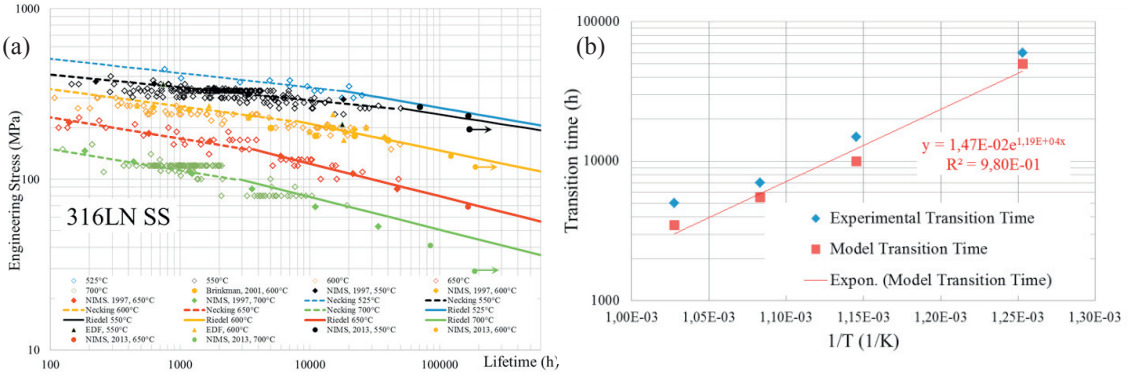

Fig. 3. (a) Comparisons between experimental lifetimes (CEA/EDF/Creusot-Loire; NIMS, (1997 & 2013), Brinkman (2001)) and the lifetimes predicted by the necking model and the Riedel model. (b) The transition time is defined by the intersection of the necking and Riedel models predicted lifetimes, comparison with observed lifetimes.

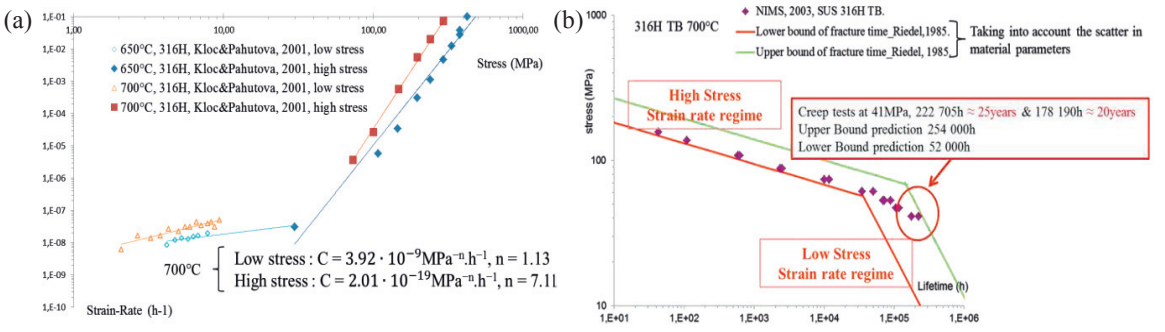

Fig. 4. (a) Minimum creep rate as function of the applied stress (after Kloc et al. 2001). (b) Comparisons between experimental lifetimes (NIMS, 2003) and the lifetimes predicted by the Riedel model at 700°C based on experimentally measured stationary creep strain rates (Fig. 4a).

Lifetimes are predicted fairly well for long term creep failure, up to 10^5h, whatever the considered austenitic stainless steels (316LN, 304H, 316H, and 321H). Their experimental data are provided by NIMS. In case of 316H and for very long term creep tests (>10^5h), at 700°C, the Riedel model differs from the experimental one. It was observed for 316L(N) steels as well (Fig. 3a). The plot of the strain rate depending on stress drawn for 316H (Kloc et al. 2001) shows that a change of slope between low and high stress regimes appears (Fig. 4a). The transition from power-law creep with a stress exponent of about 7 to a viscous creep regime occurs at a stress of about 30 MPa at 700°C. Any extrapolation from the power-law creep regime to stresses below 30 MPa may lead to serious underestimation of the creep rate and therefore overestimation of lifetime because of the nucleation law (Eq. 2). As the strain rates measured at low stress are used as inputs of the Riedel model (Eq. 3), the long term creep lifetimes are more correctly predicted.

5. Summary and conclusions

The creep fracture of 316L(N) austenitic stainless steels has been studied both experimentally and theoretically for temperatures between 525°C to 700°C and lifetimes up to nineteen years. The present study shows the followings:

1. For short term creep, failure is due to necking. Experimental lifetimes are bounded by the lower and upper bound predictions based on a necking model evolution and scatter in input parameters. This model leads to fair predictions of lifetimes up to a few thousand hours at very high temperature.
2. The transition observed in the failure curve is due to intergranular cavitation based on our FEG-SEM observations. Lifetimes are predicted fairly well for long term creep failure whatever the considered austenitic stainless steels (316LN, 304H, 316H, 321H) and the applied temperatures (525°C - 700°C). Taking into account low and high stress regimes of Norton-power law, the Riedel model allows us to predict the experimental creep lifetime data even up to 25 years for high temperature and low stress. No fitted parameter has been used. But the nucleation rate should be measured using FEG-SEM observations. This shows that the prediction of the nucleation rate is the main remaining problem to be solved for getting physically based and reliable long term lifetime predictions.

Acknowledgements

The authors wish to thank Dr. F. Abe, NIMS Invited Researcher, and the Japan Institute NIMS, for providing the creep rupture data of 18Cr-12Ni-Mo-middle N-low C. Thanks are also due to I. TOURNIER, S. VINCENT, V. RABEAU and F. BARCELO for their help and suggestions on preparing creep rupture tests and FEG-SEM observations. AREVA and EDF are also acknowledged for their support. The authors would like also to thank the project MASNA and its CEA leader, Céline CABET.

References

Auzoux, Q., 2004. Reheat cracking of austenitic stainless steels – influence of work hardening on intergranular damage. PhD thesis, MINES ParisTech and CEA Sacaly.

Brinkman C.R., 2001. Elevated-temperature mechanical properties of an advanced type 316 SS. Journal of Pressure Vessel Technology, 123.

CEA, EDF, Creusot-Loire, 1987. Protocole : étude des caractéristiques mécaniques à chaud de quatre tôles en acier inoxydable austénitique 17-12 au Mo, à très bas C et N contrôlé, in French.

Considère, M., 1885. Mémoire sur l'emploi du fer et de l'acier dans les constructions. Annales des Ponts et chaussées 9 : 574, in French.

Dumoulin, S., Tabourot, L., Chappuis, C., Vacher, P., Arrieux, R., 2003. Determination of the equivalent stress – equivalent strain relationship of a copper sample under tensile loading. J Mater Process Technol, 133:79 – 83.

Dyson, B.F., 1983. Continuous cavity nucleation and creep fracture. Scripta Metallurgica, 17 (1), 31–37.

Hart, E.W., 1967. Theory of the tensile test. Acta Metallurgica, 15 (2), 351–355.

Kloc, L., Skienicka, V., Ventruba, J., 2001. Comparison of low stress creep properties of ferritic and austenitic creep resistance steels. Materials Science and Engineering, A139-321:774-778.

Lim, R., 2011. Numerical and experimental study of creep of Grade 91 steel at high temperature. PhD thesis, MINES ParisTech and CEA Saclay.

Lim, R., Sauzay, M., Dalle, F., Tournier, I., Bonnaillie, P., Gourgues-Lorenzon, A.F., 2011. Modeling and experimental study of the tertiary creep stage of grade 91 steel. Int J Frac, 169:213-228.

Morris, D.G., Harries, D.R., 1978. Creep and rupture in type 316 stainless steel at temperatures between 525 and 900°C, Part I, II and III. Metal Science, 12 (11), 532–541.

Needleman, A., Rice, J.R., 1980. Plastic creep flow effects in the diffusive cavitation of grain boundary. Acta Metallurgica, 28 (10), 1315–1332.

NIMS, 1997 and 2013. Creep data sheet, No. M-10, 'Micrographs and microstructural characteristics of crept specimens of 18Cr-12Ni-Mo-middle N-low C hot rolled stainless steel plate (SUS 316HP), Japan.

NIMS, 1999. Creep data sheet, No. M-1, 'Micrographs and microstructural characteristics of crept specimens of 18Cr-8Ni stainless steel for boiler and heat exchanger seamless tubes (SUS 304H TB), Japan.

NIMS, 2003. Creep data sheet, No. M-2, 'Micrographs and microstructural characteristics of crept specimens of 18Cr-12Ni-Mo stainless steel for boiler and heat exchanger seamless tubes (SUS 316H TB), Japan.

NIMS, 1997. Creep data sheet, No. M-3, 'Micrographs and microstructural characteristics of crept specimens of 18Cr-10Ni-Ti stainless steel for boiler and heat exchanger seamless tubes (SUS 321H TB), Japan.

Perkins, R.A., Padgett, R.A., Anod, J.R., Tunali, N.K., 1973. Metallurgical transactions, 4:2535-2540.

Raj, R., Ashby, M.F., 1975. Intergranular fracture at elevated temperature. Acta Metallurgica, 23(6):653-666.

Riedel, H., 1987. Fracture at high temperatures. Springer-Verlag Berlin Heidelberg, New York, ISBN 0-387-17271-89.

Yoshida, M, 1985. Intergranular creep damage in 17Cr-12Ni stainless steel: Quantitative study - the role of multiaxial stress. PhD thesis, Centre des matériaux de l'école de MINES de Paris.